frontiers | Frontiers in Materials

TYPE Original Research
PUBLISHED 12 December 2024
DOI 10.3389/fmats.2024.1496162

OPEN ACCESS

EDITED BY
Bruce Pound,
Exponent , United States

REVIEWED BY
Tuba Unsal,
Istanbul University, Türkiye
Erwan Diler,
Institute De La Corrosion, France

*CORRESPONDENCE
Roberta Amendola,
roberta.amendola@montana.edu

RECEIVED 13 September 2024
ACCEPTED 25 November 2024
PUBLISHED 12 December 2024

CITATION
Acharjee A, Keskin Y, Peyton BM, Fields MW and Amendola R (2024) Effect of surface roughness on the microbiologically influenced corrosion (MIC) of copper 101. *Front. Mater.* 11:1496162.
doi: 10.3389/fmats.2024.1496162

Effect of surface roughness on the microbiologically influenced corrosion (MIC) of copper 101

Amit Acharjee[1,2], Yagmur Keskin[3,2], Brent M. Peyton[3,2], Matthew W. Fields[2,4,5] and Roberta Amendola[1,2]*

[1]Department of Mechanical and Industrial Engineering, Montana State University, Bozeman, MT, United States, [2]Center for Biofilm Engineering, Montana State University, Bozeman, MT, United States, [3]Department of Chemical and Biological Engineering, Montana State University, Bozeman, MT, United States, [4]Department of Microbiology and Cell Biology, Montana State University, Bozeman, MT, United States, [5]Department of Civil Engineering, Montana State University, Bozeman, MT, United States

The effect of varying surface roughness on microbiologically influenced corrosion by a model sulfate reducing bacterium *Oleidesulfovibrio alaskensis* G20 culture on copper 101 coupons was investigated using microscopic, spectroscopic and surface characterization techniques. After 7-day of anoxic exposure abundant biodeposits consisting of sessile cells and copper sulfide minerals were found and pitting attack was observed upon their removal. Results showed that the distribution and thickness of the biodeposits as well as the pitting severity were affected by the varying surface roughness. A direct relationship between surface roughness and microbial activity was not observed. However, a statistically significant reduction in the corrosion rate was recorded when the surface roughness was decreased from ~2.71 μm to ~0.006 μm.

KEYWORDS

copper, roughness, microbial corrosion, biofilm, sulfate-reducing bacteria, pitting corrosion

1 Introduction

Corrosion is a physico-chemical metal deterioration process that progresses in a series of redox reactions (anodic oxidation, cathodic reduction) where pure metals and/or their alloys undergo a chemical change from ground to an ionized state due to transfer of electrons from the metal to an external acceptor. When microbial cells and/or products of their metabolism such as extracellular polymeric substances (EPS) (Davidova et al., 2021; Wang et al., 2022; Li et al., 2023) are involved in deterioration, the process is termed microbiologically-influenced corrosion (MIC) (Beech and Gaylarde, 1999; Chen et al., 2014; Dou et al., 2018; Wang et al., 2020; Knisz et al., 2023; Xu et al., 2023). Although microbial communities implicated in MIC of metallic materials are diverse, significant contribution is attributed to anaerobic sulfide producing microorganisms, including sulfate-reducing bacteria (SRB). The latter are ubiquitous in aquatic and terrestrial environments, and have been associated with approximately 50% of all reported MIC-related cases (Lee et al., 1995; Yuan et al., 2013). The predominant type of damage associated with MIC and accepted as a MIC signature is pitting corrosion (Pope and Morris, 1995; Sarioğlu et al., 1997). This form of attack can severely compromise mechanical properties of the material and result in catastrophic failures (Board, 2003).

Owing to their excellent mechanical, thermal and electrical properties along with superior corrosion resistance, copper and its alloys are widely used in many systems that are installed in fresh water and marine habitats. In addition, because copper is widely used as an antimicrobial agent it has been long believed to be MIC-resistant. This assumption proved to be incorrect as it has been documented that copper-based materials are not immune to MIC (Videla and Characklis, 1992; Mansfeld et al., 1994; Geesey et al., 2000; Reyes et al., 2008; Amendola and Acharjee, 2022; Guo et al., 2022).

Reports on copper corrosion in the presence of biofilms comprised of complex bacterial communities, where a Cu_2S mineral layer was found to be deposited as the main corrosion product, implicated SRB to play a significant role (Trevors and Cotter, 1990; Angell and Chamberlain, 1991; Chen et al., 2014; Güngör et al., 2015; Huttunen-Saarivirta et al., 2016; Dou et al., 2018; Wang et al., 2020). The reactivity of copper in the presence of sulfide is well documented (Chen et al., 2010; 2017; King et al., 2017) therefore, sulfidogenic microbiomes where hydrogen sulfide (HS^-) is one of the key metabolites, pose a considerable threat to copper-based materials. While different mechanisms are proposed to explain MIC of copper and its alloys, metabolite MIC (M-MIC) has recently been accepted as the most likely cause (Dou et al., 2018; 2020; Wang et al., 2020).

In SRB-harboring biofilms, when sulfate is present, hydrogen sulfide (HS^-) is the final product of SRB metabolism. The availability of (HS^-) ions to react with Cu(I) ions governs the development of Cu_2S mineral deposits according to the reaction Equations 1, 2 (Chen et al., 2010; Chen et al., 2011; Chen et al., 2017):

$$Cu^+ + HS^- \rightarrow Cu(HS)_{ads} + e^- \quad (1)$$

$$Cu + Cu(HS)_{ads} + HS^- \rightarrow Cu_2S + H_2S + e^- \quad (2)$$

Studies conducted under abiotic conditions, *i.e.*, without any presence of microorganisms, demonstrated that for metallic materials able to develop a passive layer such as copper and stainless steel, surface roughness significantly influences the corrosion behavior; in general, a decrease in surface roughness was found to improve the corrosion resistance (Burstein and Pistorius, 1995; Li and Li, 2006; Abosrra et al., 2009; Hu et al., 2020). While the effect of surface finishing on MIC has been documented for steel, there are scarce, if any, reports pertinent to copper.

Recently, novel approaches that explore modulation of surface properties, including roughness, were proposed (Sun et al., 2020; Caro-Lara et al., 2022; Razavipour et al., 2022; Wei et al., 2022) to enhance copper antimicrobial properties and decrease microbial attachment. The effect of such treatments on copper MIC has been addressed in oxygenated environments (Sun et al., 2020; Caro-Lara et al., 2022; Wei et al., 2022) while the effectiveness of these approaches under anoxic conditions and in the presence of SRB remains limited (Wei et al., 2022).

This work studied the effect of surface roughness on copper corrosion exposed to biogenically produced hydrogen sulfide by a model SRB, *Oleidesulfovibrio alaskensis* G20 which is a sulfate-reducing, Gram-negative, vibrio-shaped bacterium capable of enzymatically reducing sulfate to hydrogen sulfide (H_2S), enabling the bacteria to respire in anoxic environments. The objective was to offer insights into the early interaction between surface topography, microbial presence, and corrosion product development. Techniques of 3D optical profilometry, Field Emission Scanning Electron Microscopy (FE-SEM), X-ray Diffraction Analysis (XRD) and EDX X-ray attenuation pit depth analysis were used to investigate corrosion morphology and product development. Corrosion rates were calculated according to the ASTM Standard G1-03 (ASTM G1-03, 2017) e1, Standard Practice for Preparing, Cleaning, and Evaluating Corrosion Test Specimens, 2017).

2 Materials and methods

2.1 Preparation of copper coupons

Coupon finishes were selected based on the roughness attainable in standard machining operations under traditional (*i.e.*, milling) and non-traditional processes (*i.e.*, superfinishing) (Grzesik et al., 2010). Pure 101 copper (Cu) (ThyssenKrupp batch# 91V3461, Cu >99.99%wt. with Oxygen <0.0005%wt. and other trace elements) was purchased from Online Metals (Seattle, WA). Coupons were cut from a bar to the dimensions of 10 × 10 × 2mm using electrical discharge machining (EDM) process to minimize defects such as mechanical deformation that may later influence the corrosion behavior. Coupons were then ground and polished on both sides to four different surface finishes: 400 US grit, 600 US grit, 800 US grit and 3-micron diamond suspension polishing using metallographic procedures with an Allied High Tech MetPrep 3 Grinder/Polisher equipped with a PH3 power head. During the surface grinding and polishing processes, copper mechanically deformed primarily through dislocation motion because of its face-centered cubic (FCC) crystal structure characterized by a high number of slip planes. The deformation associated with each surface finish may have contributed to the development of dislocation' "forests". However, previous research on FCC metals demonstrated that, over a wide range of strains, the interaction between forest and mobile dislocations only marginally increased the forest density (Csanádi et al., 2011). For this reason, the degree of deformation introduced by the preparation process was expected not to influence the corrosion behavior of the copper coupons.

Coupons without any surface modification ("as received") were also used for comparison. To remove any polishing residue, ultrasonic cleaning was performed in a two-step process with 100% acetone (Fisher Chemical Lot#187993) and 100% methanol (Fisher Chemical Lot#217743) for 10 min each. Prior to abiotic and biotic exposures, all coupons were prepared in a biosafety cabinet by dipping in ethanol solution (70% v/v) prepared with pure ethyl alcohol (Sigma-Aldrich Lot # SHBL 3646) and sterile nanopure water. This step was followed by exposure to UV light for 30 min for each side of the sample during drying in a biosafety cabinet (Ha and Ha, 2010; Guridi et al., 2019; Raeiszadeh and Adeli, 2020).

2.2 Inoculum preparation and batch exposure

The microorganism selected for this study *Desulfovibrio alaskensis* G20 was originally isolated from a soured oil reservoir

(Feio et al., 2004) and recently reclassified to *Oleidesulfovibrio alaskensis* G20 (Waite et al., 2020). *Oleidesulfovibrio alaskensis* G20 has been extensively studied due to its role in MIC and its versatile metabolic capabilities (Wikieł et al., 2014; Nair et al., 2015; Chilkoor et al., 2018; Krantz et al., 2019; Mehta-Kolte et al., 2019; Singh et al., 2022), therefore making this strain a model organism for studying corrosion of metals by SRB.

The anoxic bacterial growth medium (LS4D) was prepared with 10.39 g/L PIPES buffer disodium salt (Sigma-Aldrich #P3768), 1.63 g/L $MgCl_2{\cdot}6H_2O$ (Research Products International M24000, 1.07 g/L NH_4Cl, 0.09 g/L (Sigma-Aldrich #A9434). $CaCl_2{\cdot}2H_2O$, 0.64 mg/L (Research Products International C36200) as previously described (Mukhopadhyay et al., 2006). The LS4D growth medium was designed to minimize precipitate formation, maximize growth, and allow for optical density OD600 measurements of growth under sulfate-reducing environments and has been used under numerous growth conditions (Klonowska et al., 2008; Borglin et al., 2009; Holman et al., 2009; Zhou et al., 2015). The pH of the medium was adjusted to 7.2 using a 2 M solution of HCl and 14 mL was anaerobically dispensed into each 25 mL Balch tube. The tubes were flushed with N_2/CO_2 (80%/20%), sealed with a butyl-rubber stopper, crimped with an aluminum cap, and autoclaved. A total volume of 0.24 mL sterilized pre-mix solution containing 0.01 mL of Thauers vitamins, 0.19 mL of trace minerals, and 0.03 mL of 1M potassium phosphate solution was added to each tube after sterilization. The experiments were conducted under an electron donor and acceptor balanced condition that uses 60 mM lactate:30 mM sulfate as previously described (Franco et al., 2018; Krantz et al., 2019). Resazurin (0.1% v/v) was also added to the medium solution to serve as a general indicator of the oxidative-reduction potential (ORP) (Clark et al., 2006; Krantz et al., 2019).

For both abiotic and biotic exposures, three coupons for each surface finish were anaerobically placed in sterile growth medium in Balch tubes using a biosafety cabinet with sparging of sterile N_2 gas. The tubes were then sealed with a sterile rubber stopper and crimped with an aluminum seal cap. Blank coupon tubes were co-incubated to verify sterility during coupon processing. For biotic copper coupon exposures, *O. alaskensis* G20 was cultivated in previously prepared anaerobic tubes with LS4D medium for 3 days at 30°C and 0.1–0.2 mL of the culture was inoculated into each prepared tube containing the medium with one copper coupon. The optical density (600 nm) was measured using a Thermo Scientific, Genesys 10S UV-VIS Spectrophotometer as previously reported (Caffrey and Voordouw, 2010; Gao et al., 2016; Dong et al., 2023). For abiotic exposures, copper coupons of the as received and of each surface finish were also anaerobically exposed to sterile LS4D media in 25 mL Balch tubes to assess if any corrosion or surface deterioration occurred over the test period.

2.3 Coupon harvesting

After 7 days of exposure, aluminum seal caps and stoppers were removed from the abiotic and biotic tubes inside a fume hood and the coupons were immediately placed in vacuumed tubes for further analysis after rinsing with sterile, anoxic medium. A ZEISS SUPRA 55VP FE-SEM microscope (Carl Zeiss Microimaging, GmbH, Gottingen) was used for the enumeration of SRB sessile cells. Representative triplicates of FE-SEM images of biotically exposed copper coupons were selected for each surface finish. Three 10 × 10 μm areas were randomly chosen per each image for the quantitative evaluation of sessile SRB cell by direct surface counts. The recorded values were then extrapolated to obtain the cell density for 100 mm^2 corresponding to the coupons' total surface area. The abiotic control coupons (prepared the same way but not inoculated with *O. alaskensis* G20) did not demonstrate any microbial presence therefore no interfering species were introduced during the preparation and exposure processes. Removal of *O. alaskensis* G20 surface-associated cells and of any corrosion product resulting from the biotic exposures was performed by ultrasonic cleaning with hydrochloric acid (HCl) (Fisher Chemical Lot#179019) for 1 min as (ASTM G1-03, 2017)e1, Standard Practice for Preparing, Cleaning, and Evaluating Corrosion Test Specimens, 2017). FE-SEM analyses and weight loss measurements were performed to confirm that this procedure did not introduce any weight change or additional surface damage.

2.4 Surface analysis, determination of pit depth and mineral layer composition

Prior to abiotic and biotic exposures the as received and all prepared copper coupons were analyzed using a Filmetrics Profilm 3D Optical Profilometer to evaluate the surface topography and the distribution of asperities, defined by the peaks' height and valleys' depth. Three area roughness parameters were measured, namely, the arithmetical mean height (Sa), the root mean square height (Sq) and the maximum valley depth (Sv). Samples did not need any further preparation and white light beam setting was used for all profilometer analysis. The HCl cleaning process described previously was performed prior to FE-SEM imaging following biotic exposure while no additional steps were taken for abiotically exposed samples.

To assess the distribution, thickness, and morphology of the formed mineral layers, analysis of metallographically prepared cross sections was also performed for all exposed samples. Polishing was conducted up to 1 micron diamond suspension using Allied High Tech MULTIPREP Polishing system. EDX (Princeton Gamma-Tech, Inc, Rocky Hill, NJ) was used to evaluate the pit depth using the X-ray attenuation methodology (Avci et al., 2015). To characterize the developed mineral layer, grazing incidence X-Ray diffraction GI-XRD analysis at a grazing incidence angle of 0.8° was performed using Bruker Nano Analytics D8 Advance XRD on all coupons after the biotic exposure experiments and prior to HCl cleaning. Statistical analysis of corrosion rates and pit depth from the biotic exposure experiments was carried out using MiniTab 21.4 (MiniTab, LLC). Statistical significance was determined via Tukey simultaneous tests for differences of means to determine the effects of each surface finish.

2.5 Corrosion rates

The corrosion rates for all surface finishes were calculated from the weight loss measurement, as per ASTM Standard G1-03, using Equation 3 (ASTM G1-03, 2017)e1, Standard Practice for Preparing, Cleaning, and Evaluating Corrosion Test Specimens, 2017). Weight

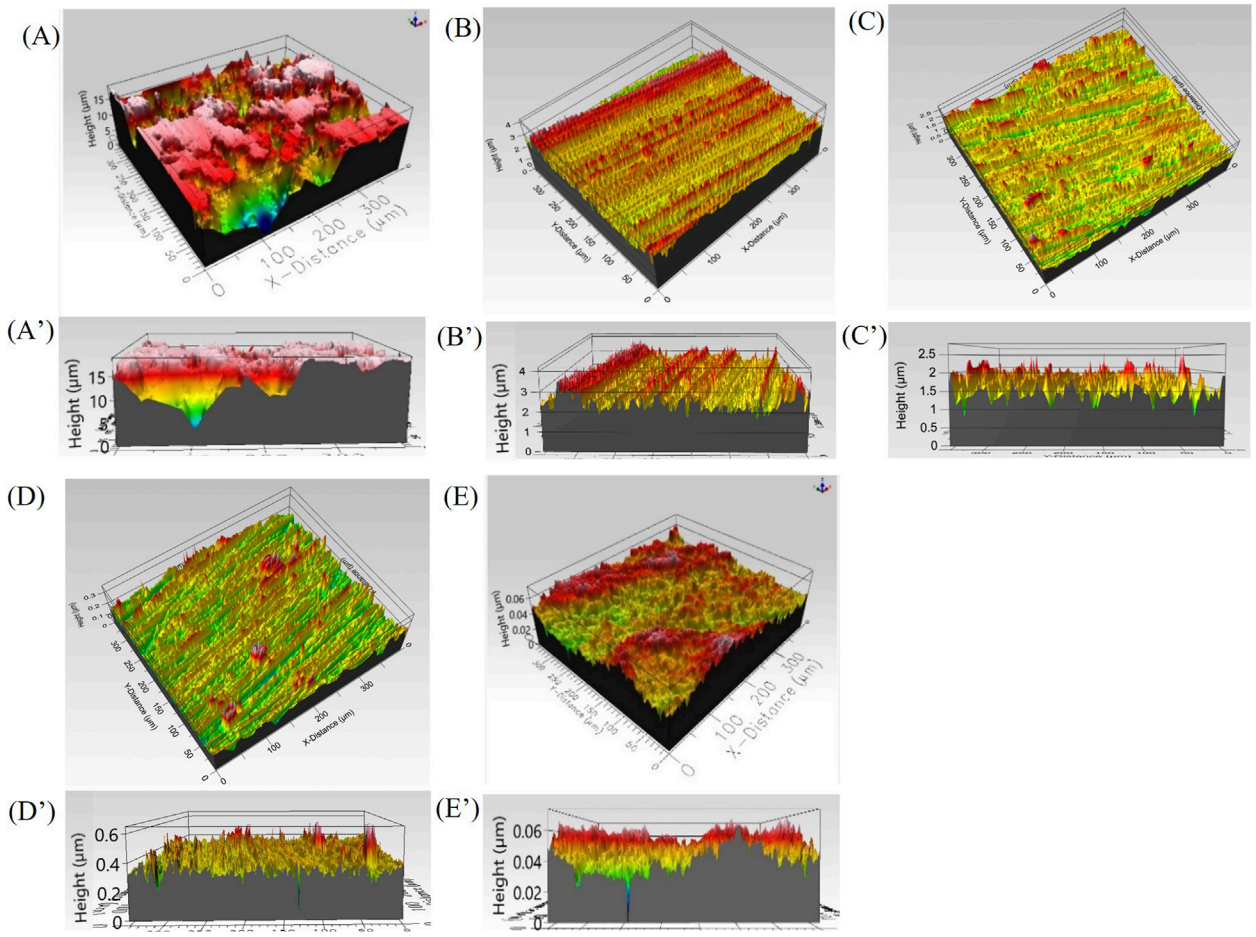

FIGURE 1
3D optical profilometer topography of copper coupons prepared with different surface finish and corresponding distribution of asperities **(A, A′)** as received, **(B, B′)** 400 US grit, **(C, C′)** 600 US grit **(D, D′)** 800 US grit, **(E, E′)** 3 µm diamond suspension polishing.

loss measurements were performed by weighing the coupons before biotic exposure and after HCl cleaning as described in Section 2.3.

$$Corrosion\ Rate\left(\frac{mm}{year}\right) = \frac{8.76 \times 10^4 \times Mass\ loss(g)}{Area\,(cm^2) \times Time\ of\ exposure\,(hours) \times Density\left(\frac{g}{cm^3}\right)} \quad (3)$$

2.6 Relative pitting severity (RPS)

RPS was used to comprehensively quantify corrosion accounting for any weight loss due to uniform corrosion. Despite being recognized as the "MIC signature", if only pitting corrosion was considered, the overall corrosion severity would be underestimated. Pit depth would in fact be measured from the corroded surface instead of the uncorroded one. Hence, both pit depth and weight loss should be used to properly describe corrosion severity. RPS defined as the ratio of pit growth rate to uniform corrosion rate based on specific weight loss was calculated from Equation 4 (Dou et al., 2018)

$$RPS = \frac{average\ maximum\ pit\ depth\,(cm) x\ metal\ density\left(\frac{g}{cm^3}\right)}{average\ specific\ weight\ loss\left(\frac{g}{cm^2}\right)} \quad (4)$$

The calculated RPS values were then used to reflect the relative importance of pitting corrosion to uniform corrosion as follows:

- RPS ≫ 1, pitting corrosion is much more severe than uniform corrosion
- RPS ≈ 1, pitting corrosion and uniform corrosion are equally important
- RPS ≪ 1, uniform corrosion is much more severe than pitting corrosion

3 Results

3.1 Optical profilometry

The 3D topography and corresponding distribution of asperities for all prepared surfaces before biotic exposures, is shown in Figures 1A–E while the Sa, Sq and Sv values are summarized in Table 1The same decreasing trend was observed for all the measured roughness parameters. The as-received samples were characterized by random distribution of surface features most likely related to the manufacturing process of the copper bars

10.3389/fmats.2024.1496162

TABLE 1 Copper coupons surface roughness parameters: arithmetical mean height (Sa), root mean square height (Sq) and maximum valley depth (Sv) measured for different surface finishes before biotic exposure to *Oleidesulfovibrio alaskensis G20* for 1 week.

Surface finish	Sa	Sq	Sv
As Received	2.71 ± 0.47	3.34 ± 0.45	12.94 ± 0.48
400 US	0.39 ± 0.12	0.49 ± 0.14	2.95 ± 0.6
600 US	0.19 ± 0.02	0.25 ± 0.02	1.23 ± 0.17
800 US	0.02 ± 0	0.03 ± 0	0.1 ± 0.02
3-micron	0.006 ± 0	0.008 ± 0	0.06 ± 0.02

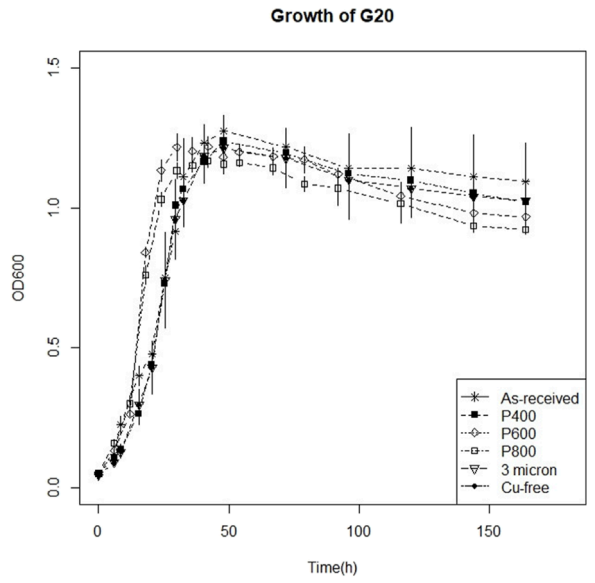

FIGURE 2
1-week growth curve of *Oleidesulfovibrio alaskensis* G20 on as received, 400 US grit, 600 US grit, 800 US grit, 3 µm diamond suspension polishing and in copper free sterile medium.

(Figure 1A). A homogeneous distribution of unidirectional grinding marks with asperities decreasing in size with increasing US grit values (Figure 1B′-1D′) was observed for the 400, 600 and 800 US grit (Figures 1B–D) and was supported by the measured values of Sv and Sq (Table 1). The 3 µm diamond suspension polished samples had a uniform distribution of asperities in the range 0.03–0.07 µm (Figure 1E′). For surfaces finished with the 800 US grit and 3 µm diamond suspensions the roughness values were below the average cell size of *O. alaskensis* G20.

3.2 Microbial growth

The *O. alaskensis* G20 planktonic growth in the presence of the copper coupons with different surface finishes over the exposure period is presented in Figure 2. The lack of significant difference in the planktonic growth of *O. alaskensis* G20 between cultures cultivated with and without copper coupons and the abundant presence of sessile cells (Figures 3A–E) indicated that, irrespective of surface finish, the levels of Cu(I) ions released by copper coupons were not toxic to either planktonic or sessile *O. alaskensis* G20 cells.

3.3 FE-SEM and GI-XRD analyses

FE-SEM imaging of copper coupons after 1-week of abiotic exposure to sterile medium, revealed unaltered surfaces (Supplementary Figure S1) with topographies like those observed using 3D optical profilometry prior to biotic exposures (Figures 1A–E). Surfaces of the exposed as-received copper coupons demonstrated the presence of dense crystalline deposits and numerous associated SRB cells (Figure 3A). The 400 US grit finished coupons were characterized by a random distribution of individual crystals varying in size (Figure 3B). For the 600 US grit, 800 US grit and 3 µm diamond suspension finished surfaces, the morphology of individual crystals regions was similar to that seen on the 400 US grit finish along with dense mineral regions with a morphology comparable to the as-received samples (Figures 3C–E). Smaller size crystals were detected in both regions for the 3 µm diamond suspension surface finish, when compared to crystal sizes measured on surfaces with higher roughness values (Figure 3E). Spectra obtained with GI-XRD demonstrated the prevalence of copper (I) sulfide (Cu_2S, chalcocite) minerals in all biodeposits, irrespective of the surface finish (Figure 4).

Irrespective of the surface finish, FE-SEM cross-sectional imaging of biodeposits demonstrated a continuous mineral layer spreading over the copper surface, decorated with scattered individual copper (I) sulfide crystals with a size varying from 3 µm to 7 µm. (Supplementary Figure S2). The thickness of the layer decreased with the surface roughness, measuring approximately 3 µm, 2 µm, 1.6 µm, 1.2 µm, 0.5 µm on the as received, 400, 600, 800 US grit SiC paper and 3 µm diamond suspension polished surfaces, respectively.

Using the FE-SEM enumeration procedure, sessile SRB cell counts (cells/cm^2) of 2.96 ± 0.31 × 10^7, 2.40 ± 0.27 × 10^7, 2.57 ± 0.42 × 10^7, 3.07 ± 0.42 × 10^7, 2.53 ± 0.21 × 10^7 for the as received, 400 US grit, 600 US grit, 800 US grit finished coupons and 3 µm diamond suspension polished coupons respectively was recorded (Supplementary Table S1). Based on the Tukey simultaneous test for differences of means (Supplementary Table S2) among the sessile cell counts, it was determined that the surface roughness did not have a statistically significant effect.

FE-SEM imaging of copper surfaces following the removal of biodeposits revealed uniform corrosion along with pitting attack (Figure 5). The size and distribution of pits varied with the surface finish. Nesting pits were observed for the as received and the 400 US grit finished samples with external pit diameter ranging from 3 µm to 6 µm while the internal pit diameter value was estimated to be between 1 µm and 3 µm (Figures 5A, B). For the 600 US grit and the 800 US grit finished samples, single pits with a diameter between 1 µm and 2 µm size were observed over the entire surface (Figures 5C, D). No specific trend was noted in the pit distribution. Intergranular corrosion was observed for the 3 µm diamond suspension polished surfaces; a scarce localized attack was found with pits of a diameter <1 µm being randomly distributed on the grains (Figure 5E).

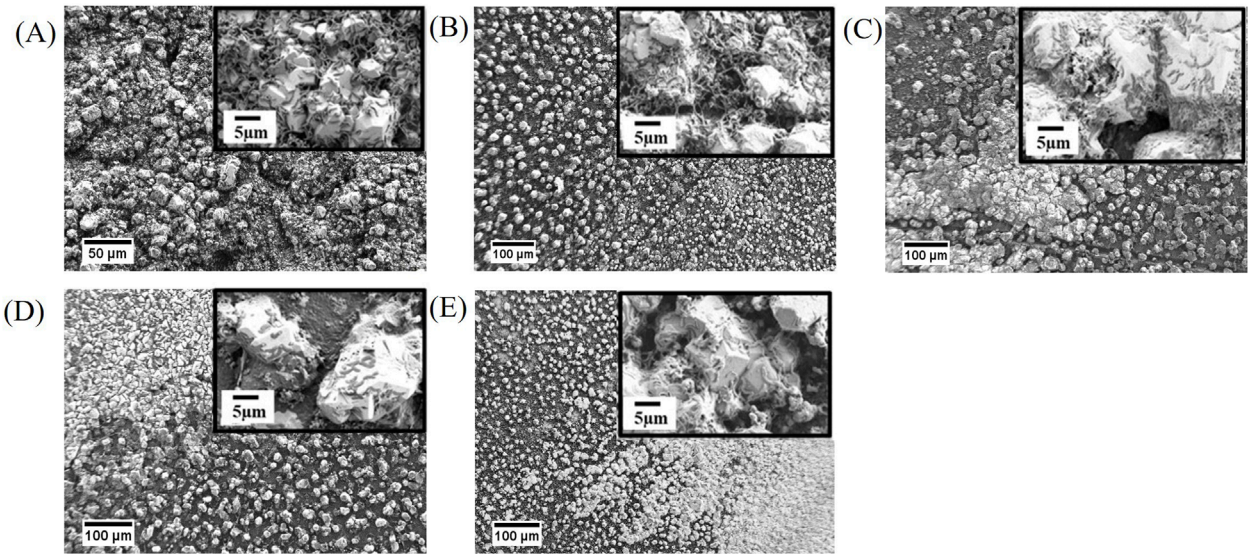

FIGURE 3
FE-SEM images of biodeposit growth on copper coupons prepared with different surface finish after 1 week of batch exposure to *Oleidesulfovibrio alaskensis* G20 **(A)** As received, **(B)** 400 US grit, **(C)** 600 US grit, **(D)** 800 US grit, and **(E)** 3 µm diamond suspension polishing.

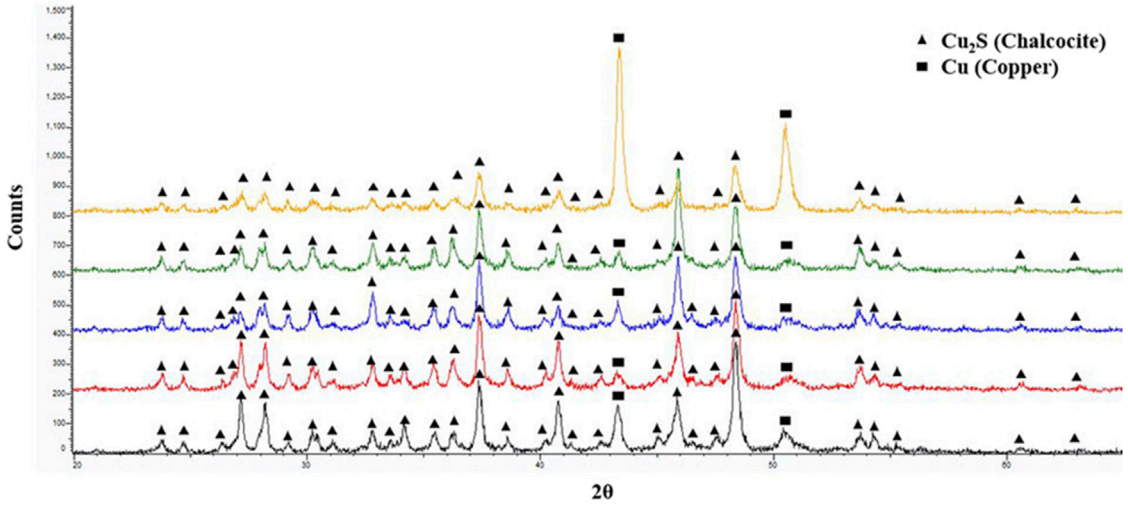

FIGURE 4
GI-XRD spectra comparison from bottom to top respectively for as received, 400 US grit, 600 US grit, 800 US grit and 3 µm diamond suspension polished coupon surface after 1-week of batch exposure to *Oleidesulfovibrio alaskensis* G20.

3.4 Corrosion rates

Table 2 summarizes the corrosion rates calculated for the 400 US grit, 600 US grit, 800 US grit finished coupons and 3 µm diamond suspension polished coupons. The number of samples tested per each surface finish is N, the "mean" is the average value of measured corrosion rate, "StDev" is the standard deviation and "95% CI" is the 95% confidence interval recorded for the as-received coupons and for each surface finish. The results indicated that a decrease in the roughness caused a decline in the overall copper corrosion rates. A reduction of 48%, 52%, 62% and 75% in corrosion rate for the 400 US grit, 600 US grit, 800 US grit finished coupons and 3 µm diamond suspension polished coupons respectively were recorded, when compared to as-received coupons. However, the Tukey simultaneous test for differences of means (Supplementary Table S3) using the corrosion rates values determined that the surface roughness Sa, did not have a statistically significant effect until it decreased from 2.71 µm (as-received samples) to 0.006 µm (3 µm diamond suspension polished samples) which corresponds to a highly finished surface (*e.g.*, superfinishing).

No weight loss was observed for abiotic 7-day exposure in sterile medium subsequently the corrosion rates could not be calculated.

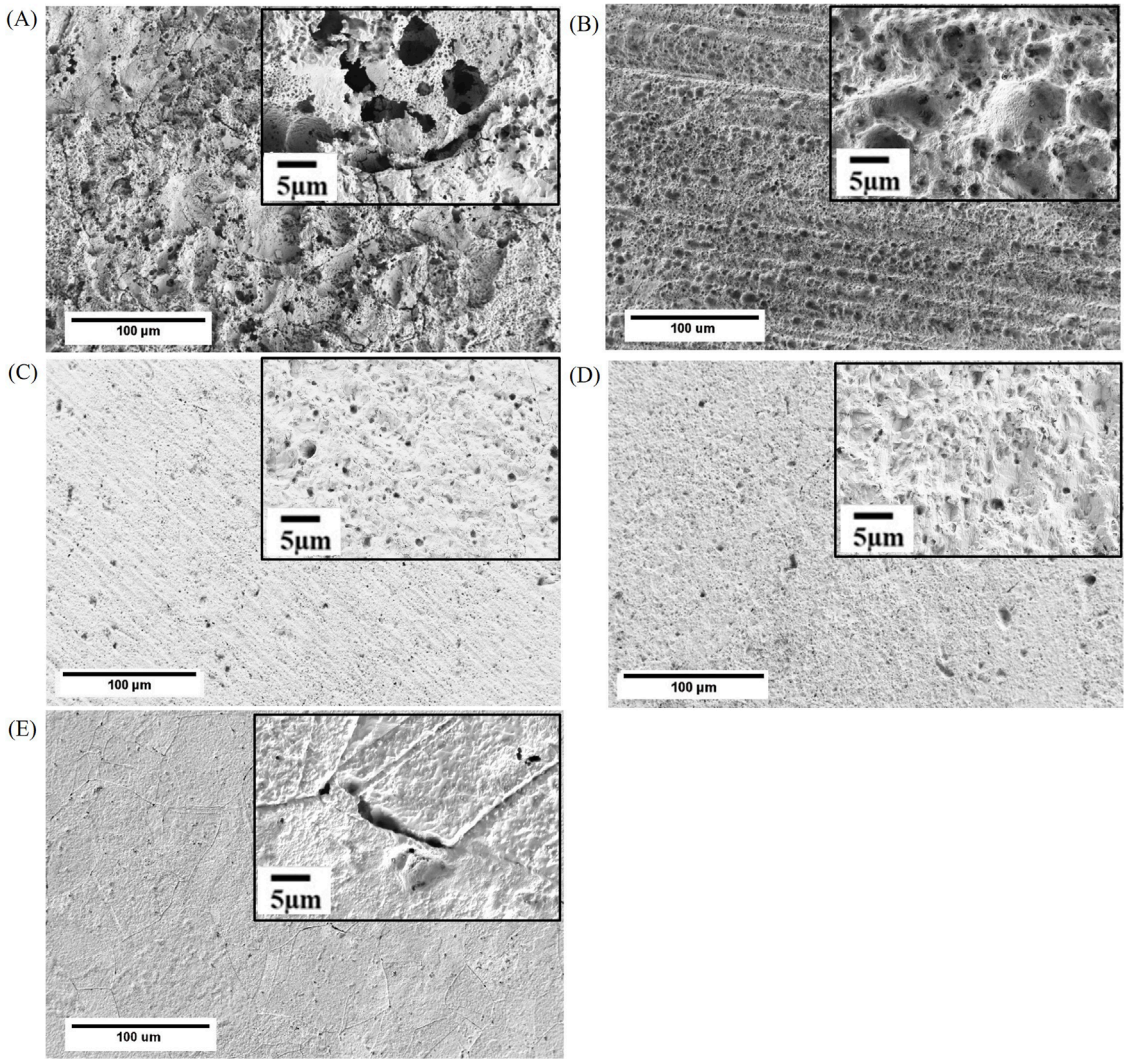

FIGURE 5
FE-SEM images of **(A)** as received, **(B)** 400 US grit, **(C)** 600 US grit, **(D)** 800 US grit, and **(E)** 3 µm diamond suspension finished coupons after removal of the biodeposit developed during 1-week batch exposure to *Oleidesulfovibrio alaskensis* G20.

3.5 Pit depth evaluation

The pit depth evaluation was carried out using the X-ray attenuation methodology in EDX spectra as previously described (Avci et al., 2015). Ten pits were randomly selected and characterized for each surface finish. A minimum of three measurements were conducted on the same pit to minimize uncertainties introduced by the X-ray production statistics. A reduction in the pit depth of 53%, 75%, 58% and 68% was recorded for the 400 US grit, 600 US grit, 800 US grit finished coupons and 3 µm diamond suspension polished samples respectively, when compared to as-received coupons (Table 3). The Tukey simultaneous test for differences of means performed on the measured pit depths, revealed that the pit depth decrease for each surface finish was statistically significant when compared to the as-received coupons. However, no specific pit depth trend was found among the surface finishes (Supplementary Table S4).

3.6 Relative pitting severity (RPS)

Table 4 shows the RPS values calculated for the 400 US grit, 600 US grit, 800 US grit finished coupons and 3 µm diamond suspension polished coupons. It was observed that, regardless of the surface finish all values were lower than 1, supporting the relative severity of uniform corrosion.

4 Discussion

The surface finish did not seem to affect the density of either planktonic or sessile SRB populations (Figures 2, 3A–E; Supplementary Table S2) but instead influenced the distribution and thickness of the biodeposits (Supplementary Figure S2), as well as the corrosion rate and morphology (Figures 5A–E). In the absence of oxygen, Cu(I) is the only available ionic form of copper that is

TABLE 2 Copper coupon corrosion rates calculated for different surface finishes after biotic exposure to *Oleidesulfovibrio alaskensis G20* for 1 week.

Surface finish	Average weight loss (mg)	Average corrosion rate (mm/year)	StDev	95% CI
As Received	7.10	0.41	0.06	(0.2659, 0.5488)
400 US grit	3.70	0.21	0.09	(0.0719, 0.3549)
600 US grit	3.30	0.19	0.19	(0.052, 0.335)
800 US grit	2.70	0.16	0.03	(0.0137, 0.2967)
3-micron diamond suspension	1.80	0.10	0.11	(-0.0387, 0.2443)

Pooled StDev = 0.109978.

TABLE 3 Pit depth measurements performed on copper coupons with different surface finishes after biotic exposure to *Oleidesulfovibrio alaskensis* G20 for 1 week.

Surface finish	N	Mean (μm)	StDev	95% CI
As Received	10	4.303	1.924	(3.597, 5.010)
400 US	10	2.028	0.478	(1.284, 2.773)
600 US	10	1.066	0.736	(0.277, 1.856)
800 US	10	1.785	0.785	(1.078, 2.491)
3micron diamond suspension	10	1.376	0.880	(0.670, 2.082)

Pooled StDev = 1.10672.

TABLE 4 RPS values calculated for copper coupons with different surface finishes after biotic exposure to *Oleidesulfovibrio alaskensis* G20 for 1 week.

Surface finish	RPS
As Received	0.55
400 US	0.49
600 US	0.29
800 US	0.59
3 micron diamond suspension	0.69

released to SRB culture media. The rate of copper corrosion would determine the concentration of free Cu(I) ions which is likely to vary between the bulk liquid and the near copper surface region. The effect of Cu(I) ions levels on its proliferation and metabolic activity responsible for sulfate reduction, and thus copper corrosion, is currently under investigation.

The distribution of asperities defined the interfacial area between the coupon and the surrounding environment. As demonstrated in the previous abiotic corrosion studies, the depth of the valleys enhanced local dissolution of material by creating micro-reaction sites and by trapping corrosion products (Burstein and Pistorius, 1995; Zuo et al., 2002). Results from this investigation demonstrated the relevance of such phenomenon in the case of copper MIC also, as the highest corrosion rate (Table 2), the thickest mineral layer (Supplementary Figure S2) and largest pits with nesting morphology (Figure 5A) were in fact observed for the as-received samples characterized by the highest surface roughness parameters (Table 1).

For the 400, 600 and 800 US grit polished coupons the gradual decrease in the roughness parameters (Table 1) resulted in a progressively smaller interfacial area available for corrosion when compared to the as-received samples. Consequently, the corrosion rate (Table 2) and the mineral layer thickness were reduced. While nesting pit morphology persisted for the 400 US grit samples (Figure 5B), for the 600 and 800 US grit coupons, the pitting attack consisted of single small diameter pits distributed over the surface (Figures 5C,D).

A 75% reduction of the corrosion rate was observed for 3 μm diamond suspension polished coupons when compared to the as-received ones (Table 2) along with the development of the thinnest mineral layer (Supplementary Figure S2). This significant decrease in corrosion rate confirmed that the negligible presence of preferential micro-reaction sites due to the flat morphology of the coupons was crucial in regulating the copper corrosion process. At the same time, the fine polishing process exposed the grain boundaries within the copper microstructure, which were otherwise "masked" by the higher roughness of all other samples. These regions, characterized by higher atomic disorder likely, caused an increase in the local chemical reactivity. Consequently, the overall pitting attack was scarce but intergranular corrosion was observed (Figure 5E).

5 Conclusion

Results of this work demonstrated that the presence of microorganisms and their metabolic activities promoted and accelerated corrosion process, since no indication of such damage through weight loss and microscopic evaluations was found after 7-day exposure in sterile (abiotic) media for any surface finishing. However, no statistically significant difference existed in the sessile cell counts regardless of the surface finishing. A direct relationship between the surface roughness and microbial activity was not identified. A 75% reduction in the corrosion rate was recorded when the surface roughness decreased from ~2.71 μm to ~0.006 μm confirming that altering surface roughness could be considered as one of the strategies aiming to mitigate MIC of copper when sulfidogenic conditions are likely to develop. However, further work is needed to potentially optimize the effectiveness of surface finishing, and to evaluate any protective capability of biodeposits for longer-term exposures.

Data availability statement

The original contributions presented in the study are included in the article/Supplementary Material, further inquiries can be directed to the corresponding author.

Author contributions

AA: Data curation, Formal Analysis, Investigation, Methodology, Writing–original draft, Writing–review and editing. YK: Data curation, Formal Analysis, Investigation, Methodology, Writing–original draft. BP: Conceptualization, Methodology, Supervision, Validation, Writing–original draft, Writing–review and editing. MF: Conceptualization, Funding acquisition, Methodology, Project administration, Supervision, Validation, Writing–original draft, Writing–review and editing. RA: Conceptualization, Methodology, Supervision, Validation, Writing–original draft, Writing–review and editing.

Funding

The author(s) declare that financial support was received for the research, authorship, and/or publication of this article. This work was financially supported by the United States National Science Foundation (NSF # 1920954), and it was performed in part at the Montana Nanotechnology Facility, an NNCI member supported by NSF Grant ECCS-2025391.

Conflict of interest

The authors declare that the research was conducted in the absence of any commercial or financial relationships that could be construed as a potential conflict of interest.

Publisher's note

All claims expressed in this article are solely those of the authors and do not necessarily represent those of their affiliated organizations, or those of the publisher, the editors and the reviewers. Any product that may be evaluated in this article, or claim that may be made by its manufacturer, is not guaranteed or endorsed by the publisher.

Supplementary material

The Supplementary Material for this article can be found online at: https://www.frontiersin.org/articles/10.3389/fmats.2024.1496162/full#supplementary-material

References

Abosrra, L., Ashour, A. F., Mitchell, S. C., and Youseffi, M. (2009). Corrosion of mild steel and 316L austenitic stainless steel with different surface roughness in sodium chloride saline solutions. *WIT Trans. Eng. Sci.* 65, 161–172. doi:10.2495/ECOR090161

Amendola, R., and Acharjee, A. (2022). Microbiologically influenced corrosion of copper and its alloys in anaerobic aqueous environments: a review. *Front. Microbiol.* 13, 806688. doi:10.3389/fmicb.2022.806688

Angell, P., and Chamberlain, A. H. L. (1991). The role of extracellular products in copper colonisation. *Int. Biodeterior.* 27, 135–143. doi:10.1016/0265-3036(91)90005-C

ASTM G1-03 (2017). "e1, Standard Practice for Preparing, Cleaning, and Evaluating Corrosion Test Specimens (2017)," in *Book of standards*. doi:10.1520/G0001-03R17E01

Avci, R., Davis, B. H., Wolfenden, M. L., Kellerman, L. R., Lucas, K., Martin, J., et al. (2015). A practical method for determining pit depths using X-ray attenuation in EDX spectra. *Corros. Sci.* 93, 9–18. doi:10.1016/J.CORSCI.2014.12.018

Beech, I. B., and Gaylarde, C. C. (1999). Recent advances in the study of biocorrosion: an overview. *Rev. Microbiol.* 30, 117–190. doi:10.1590/s0001-37141999000300001

Board (NTSB) (2003). *Natural gas pipeline rupture and fire near carlsbad*. Washington, DC.

Borglin, S., Joyner, D., Jacobsen, J., Mukhopadhyay, A., and Hazen, T. C. (2009). Overcoming the anaerobic hurdle in phenotypic microarrays: generation and visualization of growth curve data for Desulfovibrio vulgaris Hildenborough. *J. Microbiol. Methods* 76, 159–168. doi:10.1016/J.MIMET.2008.10.003

Burstein, G. T., and Pistorius, P. C. (1995). Surface roughness and the metastable pitting of stainless steel in chloride solutions. *Corrosion* 51, 380–385. doi:10.5006/1.3293603

Caffrey, S. M., and Voordouw, G. (2010). Effect of sulfide on growth physiology and gene expression of Desulfovibrio vulgaris Hildenborough. *Ant. Van Leeuwenhoek* 97, 11–20. doi:10.1007/S10482-009-9383-Y

Caro-Lara, L., Vargas, I. T., Ramos-Moore, E., Galarce, C., Diaz-Droguett, D., and Pizarro, G. E. (2022). Enhancing the contact-killing effect of copper by surface laser texturing. *J. Environ. Chem. Eng.* 10, 108497. doi:10.1016/J.JECE.2022.108497

Chen, J., Qin, Z., Martino, T., and Shoesmith, D. W. (2017). Non-uniform film growth and micro/macro-galvanic corrosion of copper in aqueous sulphide solutions containing chloride. *Corros. Sci.* 114, 72–78. doi:10.1016/J.CORSCI.2016.10.024

Chen, J., Qin, Z., and Shoesmith, D. W. (2010). Kinetics of corrosion film growth on copper in neutral chloride solutions containing small concentrations of sulfide. *J. Electrochem. Soc.* 157, C338. doi:10.1149/1.3478570

Chen, J., Qin, Z., and Shoesmith, D. W. (2011). Long-term corrosion of copper in a dilute anaerobic sulfide solution. *Electrochim. Acta* 56, 7854–7861. doi:10.1016/J.ELECTACTA.2011.04.086

Chen, S., Wang, P., and Zhang, D. (2014). Corrosion behavior of copper under biofilm of sulfate-reducing bacteria. *Corros. Sci.* 87, 407–415. doi:10.1016/j.corsci.2014.07.001

Chilkoor, G., Karanam, S. P., Star, S., Shrestha, N., Sani, R. K., Upadhyayula, V. K. K., et al. (2018). Hexagonal boron nitride: the thinnest insulating barrier to microbial corrosion. *ACS Nano* 12, 2242–2252. doi:10.1021/acsnano.7b06211

Clark, M. E., He, Q., He, Z., Huang, K. H., Alm, E. J., Wan, X. F., et al. (2006). Temporal transcriptomic analysis as Desulfovibrio vulgaris Hildenborough transitions into stationary phase during electron donor depletion. *Appl. Environ. Microbiol.* 72, 5578–5588. doi:10.1128/AEM.00284-06

Csanádi, T., Chinh, N. Q., Gubicza, J., and Langdon, T. G. (2011). Plastic behavior of fcc metals over a wide range of strain: macroscopic and microscopic descriptions and their relationship. *Acta Mater* 59, 2385–2391. doi:10.1016/J.ACTAMAT.2010.12.034

Davidova, I. A., Lenhart, T. R., Nanny, M. A., and Suflita, J. M. (2021). Composition and corrosivity of extracellular polymeric substances from the hydrocarbon-degrading sulfate-reducing bacterium desulfoglaeba alkanexedens ALDC. *Microorganisms* 9, 1994. doi:10.3390/MICROORGANISMS9091994

Dong, Y., Wang, J., Gao, Z., Di, J., Wang, D., Guo, X., et al. (2023). Study on growth influencing factors and desulfurization performance of sulfate reducing bacteria based on the response surface methodology. *ACS Omega* 8, 4046–4059. doi:10.1021/acsomega.2c06931

Dou, W., Jia, R., Jin, P., Liu, J., Chen, S., and Gu, T. (2018). Investigation of the mechanism and characteristics of copper corrosion by sulfate reducing bacteria. *Corros. Sci.* 144, 237–248. doi:10.1016/j.corsci.2018.08.055

Dou, W., Pu, Y., Han, X., Song, Y., Chen, S., and Gu, T. (2020). Corrosion of Cu by a sulfate reducing bacterium in anaerobic vials with different headspace volumes. *Bioelectrochemistry* 133, 107478. doi:10.1016/j.bioelechem.2020.107478

Feio, M. J., Zinkevich, V., Beech, I. B., Llobet-Brossa, E., Eaton, P., Schmitt, J., et al. (2004). Desulfovibrio alaskensis sp. nov., a sulphate-reducing bacterium from a soured oil reservoir. *Int. J. Syst. Evol. Microbiol.* 54, 1747–1752. doi:10.1099/IJS.0.63118-0

Franco, L. C., Steinbeisser, S., Zane, G. M., Wall, J. D., and Fields, M. W. (2018). Cr(VI) reduction and physiological toxicity are impacted by resource ratio in Desulfovibrio vulgaris. *Appl. Microbiol. Biotechnol.* 102, 2839–2850. doi:10.1007/s00253-017-8724-4

Gao, S. H., Ho, J. Y., Fan, L., Richardson, D. J., Yuan, Z., and Bond, P. L. (2016). Antimicrobial effects of free nitrous acid on Desulfovibrio vulgaris: implications for sulfide-induced corrosion of concrete. *Appl. Environ. Microbiol.* 82, 5563–5575. doi:10.1128/AEM.01655-16

Geesey, G. G., Beech, I., Bremer, P. J., Webster, B. J., and Wells, D. B. (2000). "Biocorrosion," in *Biofilms II: process analysis and applications*. Editor J. D. Bryers (Wiley-Liss, Inc.), 327–372. Available at: https://scholarworks.montana.edu/xmlui/handle/1/13401 (Accessed March 18, 2024).

Grzesik, W., Kruszynski, B., and Ruszaj, A. (2010). Surface integrity of machined surfaces. *Surf. Integr. Mach.*, 143–179. doi:10.1007/978-1-84882-874-2_5

Güngör, N. D., Çotuk, A., and Dışpınar, D. (2015). The effect of Desulfovibrio sp. biofilms on corrosion behavior of copper in sulfide-containing solutions. *J. Mater. Eng. Perform.* 24, 1357–1364. doi:10.1007/s11665-015-1388-2

Guo, N., Mao, X., Liu, T., Hui, X., Guo, Z., Tan, B., et al. (2022). Corrosion mechanism of copper in seawater containing the bacterial pyomelanin with redox activity. *Corros. Sci.* 204, 110407. doi:10.1016/J.CORSCI.2022.110407

Guridi, A., Sevillano, E., Fuente, I. de la, Mateo, E., Eraso, E., and Quindós, G. (2019). Disinfectant activity of A portable ultraviolet C equipment. *Int. J. Environ. Res. Public Heal.* 16, 4747. doi:10.3390/IJERPH16234747

Ha, J. I. H., and Ha, S.Do (2010). Synergistic effects of ethanol and UV radiation to reduce levels of selected foodborne pathogenic bacteria. *J. Food Prot.* 73, 556–561. doi:10.4315/0362-028X-73.3.556

Holman, H. Y. N., Wozei, E., Lin, Z., Comolli, L. R., Ball, D. A., Borglin, S., et al. (2009). Real-time molecular monitoring of chemical environment in obligate anaerobes during oxygen adaptive response. *Proc. Natl. Acad. Sci. U. S. A.* 106, 12599–12604. doi:10.1073/PNAS.0902070106

Hu, M., Zhang, W., Shang, X., Wen, J., Zhao, Z., Qiao, B., et al. (2020). Effect of surface roughness on copper corrosion in simulated beishan groundwater, China. *Int. J. Electrochem. Sci.* 15, 2961–2972. doi:10.20964/2020.04.05

Huttunen-Saarivirta, E., Rajala, P., and Carpén, L. (2016). Corrosion behaviour of copper under biotic and abiotic conditions in anoxic ground water: electrochemical study. *Electrochim. Acta* 203, 350–365. doi:10.1016/J.ELECTACTA.2016.01.098

King, F., Chen, J., Qin, Z., Shoesmith, D., and Lilja, C. (2017). Sulphide-transport control of the corrosion of copper canisters. *Int. J. Corros. Process. Corros. Control* 52, 210–216. doi:10.1080/1478422X.2017.1300363

Klonowska, A., Clark, M. E., Thieman, S. B., Giles, B. J., Wall, J. D., and Fields, M. W. (2008). Hexavalent chromium reduction in Desulfovibrio vulgaris Hildenborough causes transitory inhibition of sulfate reduction and cell growth. *Appl. Microbiol. Biotechnol.* 78, 1007–1016. doi:10.1007/S00253-008-1381-X

Knisz, J., Eckert, R., Gieg, L. M., Koerdt, A., Lee, J. S., Silva, E. R., et al. (2023). Microbiologically influenced corrosion—more than just microorganisms. *FEMS Microbiol. Rev.* 47, fuad041–33. doi:10.1093/FEMSRE/FUAD041

Krantz, G. P., Lucas, K., Wunderlich, E. L., Hoang, L. T., Avci, R., Siuzdak, G., et al. (2019). Bulk phase resource ratio alters carbon steel corrosion rates and endogenously produced extracellular electron transfer mediators in a sulfate-reducing biofilm. *Biofouling* 35, 669–683. doi:10.1080/08927014.2019.1646731

Lee, W., Lewandowski, Z., Nielsen, P. H., and Allan Hamilton, W. (1995). Role of sulfate-reducing bacteria in corrosion of mild steel: a review. *Biofouling* 8, 165–194. doi:10.1080/08927019509378271

Li, W., and Li, D. Y. (2006). Influence of surface morphology on corrosion and electronic behavior. *Acta Mater* 54, 445–452. doi:10.1016/J.ACTAMAT.2005.09.017

Li, Y., Gong, S., Song, C., Tian, H., Yan, Z., and Wang, S. (2023). Roles of microbial extracellular polymeric substances in corrosion and scale inhibition of circulating cooling water. *ACS ES T Water* 3, 743–755. doi:10.1021/acsestwater.2c00524

Mansfeld, F., Liu, G., Xiao, H., Tsai, C. H., and Little, B. J. (1994). The corrosion behavior of copper alloys, stainless steels and titanium in seawater. *Corros. Sci.* 36, 2063–2095. doi:10.1016/0010-938x(94)90008-6

Mehta-Kolte, M. G., Stoeva, M. K., Mehra, A., Redford, S. A., Youngblut, M. D., Zane, G., et al. (2019). Adaptation of Desulfovibrio alaskensis G20 to perchlorate, a specific inhibitor of sulfate reduction. *Environ. Microbiol.* 21, 1395–1406. doi:10.1111/1462-2920.14570

Mukhopadhyay, A., He, Z., Alm, E. J., Arkin, A. P., Baidoo, E. E., Borglin, S. C., et al. (2006). Salt stress in Desulfovibrio vulgaris hildenborough: an integrated genomics approach. *J. Bacteriol.* 188, 4068–4078. doi:10.1128/JB.01921-05

Nair, R. R., Silveira, C. M., Diniz, M. S., Almeida, M. G., Moura, J. J. G., and Rivas, M. G. (2015). Changes in metabolic pathways of Desulfovibrio alaskensis G20 cells induced by molybdate excess. *J. Biol. Inorg. Chem.* 20, 311–322. doi:10.1007/S00775-014-1224-4

Pope, D. H., and Morris, I. E. A. (1995). Some experiences with microbiologically influenced corrosion of pipelines. *Mater. Perform.* 34. doi:10.2172/793996

Raeiszadeh, M., and Adeli, B. (2020). A critical review on ultraviolet disinfection systems against COVID-19 outbreak: applicability, validation, and safety considerations. *ACS Photonics* 7, 2941–2951. doi:10.1021/acsphotonics.0c01245

Razavipour, M., Gonzalez, M., Singh, N., Cimenci, C. E., Chu, N., Alarcon, E. I., et al. (2022). Biofilm inhibition and antiviral response of cold sprayed and shot peened copper surfaces: effect of surface morphology and microstructure. *J. Therm. Spray. Technol.* 31, 130–144. doi:10.1007/s11666-021-01315-7

Reyes, A., Letelier, M. V., De la Iglesia, R., González, B., and Lagos, G. (2008). Microbiologically induced corrosion of copper pipes in low-pH water. *Int. Biodeterior. Biodegrad.* 61, 135–141. doi:10.1016/J.IBIOD.2007.06.001

Sarioğlu, F., Javaherdashti, R., and Aksöz, N. (1997). Corrosion of a drilling pipe steel in an environment containing sulphate-reducing bacteria. *Int. J. Press. Vessel. Pip.* 73, 127–131. doi:10.1016/S0308-0161(97)00022-7

Singh, R. N., Gnimpieba, E. Z., and Sani, R. K. (2022). "Challenges in single cells sequencing Microbial community and biofilm: a case of Oleidesulfovibrio alaskensis G20 NGS protocol," in *Proceedings - 2022 IEEE international conference on bioinformatics and biomedicine, BIBM 2022* (Las Vegas, NV: Institute of Electrical and Electronics Engineers Inc.), 3613–3615. doi:10.1109/BIBM55620.2022.9995610

Sun, Y., Zhang, Z., Qin, Y., Xu, X., and Yang, S. (2020). The effect of rotation accelerated shot peening on mechanical property and antimicrobial activity of pure copper. *Surf. Coatings Technol.* 384, 125319. doi:10.1016/J.SURFCOAT.2019.125319

Trevors, J. T., and Cotter, C. M. (1990). Copper toxicity and uptake in microorganisms. *J. Ind. Microbiol.* 6, 77–84. doi:10.1007/BF01576426

Videla, H. A., and Characklis, W. G. (1992). Biofouling and microbially influenced corrosion. *Int. Biodeterior. Biodegrad.* 29, 195–212. doi:10.1016/0964-8305(92)90044-O

Waite, D. W., Chuvochina, M., Pelikan, C., Parks, D. H., Yilmaz, P., Wagner, M., et al. (2020). Proposal to reclassify the proteobacterial classes Deltaproteobacteria and Oligoflexia, and the phylum Thermodesulfobacteria into four phyla reflecting major functional capabilities. *Int. J. Syst. Evol. Microbiol.* 70, 5972–6016. doi:10.1099/IJSEM.0.004213

Wang, D., Liu, J., Jia, R., Dou, W., Kumseranee, S., Punpruk, S., et al. (2020). Distinguishing two different microbiologically influenced corrosion (MIC) mechanisms using an electron mediator and hydrogen evolution detection. *Corros. Sci.* 177, 108993. doi:10.1016/j.corsci.2020.108993

Wang, Y., Zhang, R., Duan, J., Shi, X., Zhang, Y., Guan, F., et al. (2022). Extracellular polymeric substances and biocorrosion/biofouling: recent advances and future perspectives. *Int. J. Mol. Sci.* 23, 5566. doi:10.3390/IJMS23105566

Wei, B., Xu, J., Gao, L., Feng, H., Wu, J., Sun, C., et al. (2022). Nanosecond pulsed laser-assisted modified copper surface structure: enhanced surface microhardness and microbial corrosion resistance. *J. Mater. Sci. Technol.* 107, 111–123. doi:10.1016/J.JMST.2021.08.023

Wikieł, A. J., Datsenko, I., Vera, M., and Sand, W. (2014). Impact of Desulfovibrio alaskensis biofilms on corrosion behaviour of carbon steel in marine environment. *Bioelectrochemistry* 97, 52–60. doi:10.1016/J.BIOELECHEM.2013.09.008

Xu, D., Gu, T., and Lovley, D. R. (2023). Microbially mediated metal corrosion. *Nat. Rev. Microbiol.* 21, 705–718. doi:10.1038/S41579-023-00920-3

Yuan, S., Liang, B., Zhao, Y., and Pehkonen, S. O. (2013). Surface chemistry and corrosion behaviour of 304 stainless steel in simulated seawater containing inorganic sulphide and sulphate-reducing bacteria. *Corros. Sci.* 74, 353–366. doi:10.1016/j.corsci.2013.04.058

Zhou, A., Hillesland, K. L., He, Z., Schackwitz, W., Tu, Q., Zane, G. M., et al. (2015). Rapid selective sweep of pre-existing polymorphisms and slow fixation of new mutations in experimental evolution of Desulfovibrio vulgaris. *ISME J.* 911 (9), 2360–2372. doi:10.1038/ismej.2015.45

Zuo, Y., Wang, H., and Xiong, J. (2002). The aspect ratio of surface grooves and metastable pitting of stainless steel. *Corros. Sci.* 44, 25–35. doi:10.1016/S0010-938X(01)00039-7